Available online at www.sciencedirect.com

SciVerse ScienceDirect

journal homepage: www.elsevier.com/locate/he

Influence of 2-(4-chlorophenyl)-2-oxoethyl benzoate on the hydrogen evolution and corrosion inhibition of 18 Ni 250 grade weld aged maraging steel in 1.0 M sulfuric acid medium

B.S. Sanatkumar [a], Jagannath Nayak [b], A. Nityananda Shetty [a,*]

[a] Department of Chemistry, National Institute of Technology Karnataka, Surathkal, Srinivasnagar 575 025, Karnataka, India
[b] Department of Metallurgical and Materials Engineering, National Institute of Technology Karnataka, Surathkal, Srinivasnagar 575 025, Karnataka, India

ARTICLE INFO

Article history:
Received 8 February 2012
Received in revised form
22 February 2012
Accepted 27 February 2012
Available online 11 April 2012

Keywords:
Hydrogen evolution
Maraging steel
Organic inhibitor
Polarization
Impedance

ABSTRACT

Electrochemical corrosion behavior and hydrogen evolution reaction of weld aged maraging steel have been investigated, in 1.0 M sulfuric acid solution containing different concentrations of 2-(4-chlorophenyl)-2-oxoethyl benzoate (CPOB). The data obtained from polarization technique showed that the corrosion current density (i_{corr}) and the hydrogen evolution rate decrease, indicating a decrease in the corrosion rate of weld aged maraging steel as well as an increase in the inhibition efficiency (η%) with the increase in inhibitor concentration. Changes in impedance parameters were indicative of adsorption of CPOB on the metal surface, leading to the formation of protective film. Both activation (E_a) and thermodynamic parameters (ΔG^0_{ads}, ΔH^0_{ads} and ΔS^0_{ads}) were calculated and discussed. The adsorption of CPOB on the weld aged maraging steel surface obeyed the Langmuir adsorption isotherm model. Scanning electron microscopy (SEM) and energy dispersive X-ray spectroscopy (EDS) study confirmed the formation of an adsorbed protective film on the metal surface.

Copyright © 2012, Hydrogen Energy Publications, LLC. Published by Elsevier Ltd. All rights reserved.

1. Introduction

Maraging steels are a class of ultra-high strength steels developed mainly for aerospace, military, aircraft and tooling applications. The name maraging derives from "martensite-aging," referring to the heat treatment carried out to induce the precipitation of intermetallics in the Fe–Ni martensitic matrix, responsible for the excellent mechanical properties [1]. The alloy is a low carbon steel that contains about 18 wt% Ni, substantial amounts of Co and Mo, together with small additions of Ti. However, depending on the requirements of the application, the composition of the material can be modified. The high strength of maraging steel is achieved by aging the specimen at 400–500 °C, where the precipitation of intermetallics takes place [2]. Corrosion of maraging steel is a fundamental academic and industrial concern that has received a considerable amount of attention. According to the available literature, 18 Ni maraging steel, when exposed to atmosphere, undergoes more or less uniform corrosion and gets completely covered with rust [3]. Maraging steels are found to be less susceptible to hydrogen embrittlement than high-strength steels owing to significantly low diffusion of hydrogen in them [4]. Due to the variety of applications, these steels frequently come in contact with corrosive environments; the strategy is to isolate the metal from corrosive agents. The addition of inhibitors to the corrosion medium serves the purpose. Only a few reports on the corrosion inhibition of maraging steel in acid solution using organic inhibitors are available in the literature [5,6].

* *Corresponding author*. Tel.: +91 9448779922; fax: +91 824 2474033.
E-mail address: nityashreya@gmail.com (A. Nityananda Shetty).

0360-3199/$ – see front matter Copyright © 2012, Hydrogen Energy Publications, LLC. Published by Elsevier Ltd. All rights reserved.
doi:10.1016/j.ijhydene.2012.02.165

Application of corrosion inhibitors is the most economical and practical method to mitigate electrochemical corrosion. Organic substances such as heterocyclic compounds containing one or more nitrogen, oxygen, and sulfur atoms, multiple bonds in the molecule can adsorb on the metallic surface and can act by blocking the active sites or generating a physical barrier to reduce the transport of corrosive species to the metal surface [7]. These compounds are rich in heteroatoms, such as sulfur, nitrogen, and oxygen, which can be used as effective inhibitors because of their strong chemical activity. The present research is aimed at evaluating a new organic inhibitor with good inhibition efficiency against weld aged maraging steel corrosion [8].

In acidic medium, the corrosion of the metal generally involves the liberation of hydrogen as the cathodic reaction. Therefore, the inhibition of corrosion should also inhibit the hydrogen evolution. Evolved hydrogen may recombine and leave the surface as a gas or may enter the metal causing the hydrogen-induced degradation of the metal. In order to reduce the susceptibility to hydrogen uptake, the modification of solution by addition of inhibitors or the modification of the metal surface may be applied [9]. In continuation of our search for developing corrosion inhibitors with high effectiveness and efficiency, the present paper explores the use of 2-(4-chlorophenyl)-2-oxoethyl benzoate (CPOB) as corrosion inhibitor for weld aged maraging steel surface in 1.0 M sulfuric acid solution. Potentiodynamic polarization and electrochemical impedance spectroscopy (EIS) techniques were used to determine the inhibition efficiency of CPOB; and scanning electron microscopy (SEM) was used to get the surface profiles of the corroded surfaces. Energy dispersive X-ray spectroscopy (EDS) investigations were carried out in order to identify the elemental composition of the species formed on the metal surface after its immersion in 1.0 M sulfuric acid in the presence and absence of inhibitor. The effect of temperature was assessed in order to propose a suitable mechanism for hydrogen evolution and the inhibition action of CPOB on weld aged maraging steel sample.

2. Experimental

2.1. Material

The compositions of the maraging steel (18 Ni 250 grade) is as follows (wt%): C = 0.015, Ni = 18, Mo = 4.8, Co = 7.75, Si = 0.1, O = 30 ppm, H = 2.0 ppm, Ti = 0.45, Al = 0.005–0.15, Mn = 0.1, P = 0.01, S = 0.01, N = 30 ppm and the balance is Fe. The maraging steel plates of composition as mentioned above were welded by GTAW–DCSP (Gas tungsten arc welding – Direct-current straight polarity) using filler material of compositions (wt%): C = 0.015, Ni = 17, Mo = 2.55, Co = 12, Ti = 0.015, Al = 0.4, Mn = 0.1, Si = 0.1 and the balance is Fe. The specimen was taken from the plates which were welded as per above and aged at 480 ± 5 °C for 3 h followed by air cooling.

2.2. Preparation of test coupons

The working electrode was cut from the plate and sealed with epoxy resin, leaving only 0.64 cm^2 of the surface area exposed to the electrolyte. Prior to each experiment, the working electrode was mechanically polished with a fine grade of emery papers (400–2000 grade), finally on polishing wheel using legated alumina to obtain mirror finish. Then it was degreased with acetone, washed with double distilled water and dried before immersing in the corrosion medium. All the experiments were carried out at different temperatures in the open atmosphere, under unstirred conditions.

2.3. Medium

The corrosive medium was 1.0 M sulfuric acid solution prepared from analytical-reagent-grade sulfuric acid and double distilled water. Inhibitive action of CPOB on the corrosion of weld aged maraging steel in 1.0 M sulfuric acid solution was studied by introducing different concentrations of the inhibitor into the solution. The concentration range of CPOB used in this study was 0.2 mM–1.0 mM. The experiments were carried out at temperatures 30 °C, 35 °C, 40 °C, 45 °C and 50 °C (±0.5 °C), in a calibrated thermostat.

2.4. Synthesis of 2-(4-chlorophenyl)-2-oxoethyl benzoate (CPOB)

The inhibitor CPOB was synthesized as reported in the literature [10,11]. A mixture of benzoic acid (1.0 g, 0.0081 mol), potassium carbonate (1.23 g, 0.0089 mol) and 2-bromo-1-(4-chlorophenyl) ethanone (1.81 g, 0.0081 mol) in dimethylformamide (10 ml) was stirred at room temperature for 2 h. On cooling, colorless needle-shaped crystals of 2-(4-chlorophenyl)-2-oxoethyl benzoate begin to separate out. The crude product was filtered off and re-crystallized from ethanol. The product was characterized by elemental analyses, melting point (119–120 °C) and infrared spectra. The synthesis scheme is shown below.

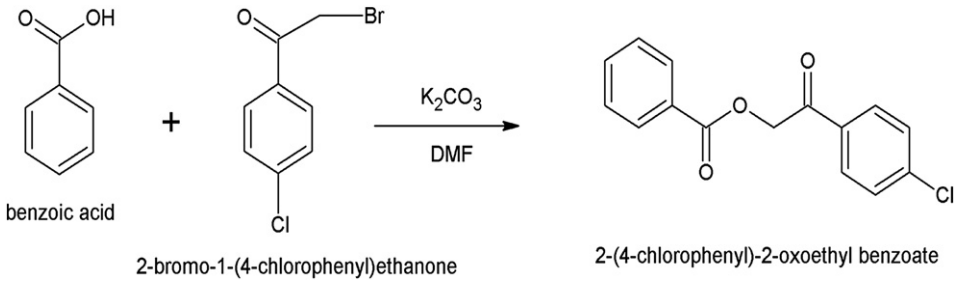

2.5. Electrochemical techniques

Electrochemical measurements were carried out using electrochemical work station, Gill AC having ACM instrument Version 5 software. The arrangement used was a conventional three-electrode compartment glass cell with a platinum counter electrode and a saturated calomel electrode (SCE) as reference. The working electrode was made of weld aged maraging steel. All the values of potential are referred to the SCE. The polarization studies were carried out immediately after the EIS studies on the same electrode without any further surface treatment.

2.5.1. Potentiodynamic polarization studies

Finely polished weld aged maraging steel specimen was exposed to the corrosion medium of 1.0 M sulfuric acid solution in the presence and absence of the inhibitor at different temperatures (30–50 °C) and allowed to establish a steady-state open circuit potential (OCP). The potentiodynamic current–potential curves were recorded by polarizing the specimen to −250 mV cathodically and +250 mV anodically with respect to the OCP at a scan rate of 1 mV s^{-1}.

2.5.2. Electrochemical impedance spectroscopy studies (EIS)

The impedance measurements were carried out in the frequency range of 10 kHz to 0.01 Hz, at the rest potential, by applying 10 mV sine wave AC voltage. The double-layer capacitance (C_{dl}), the charge-transfer resistance (R_{ct}), film capacitance (C_f) and film resistance (R_f) were calculated from the Nyquist plot.

In all the above measurements, at least three similar results were considered, and their average values are reported.

2.6. SEM/EDS investigations

The surface morphology of the weld aged maraging steel specimen immersed in 1.0 M sulfuric acid solution in the presence and absence of inhibitor were compared by recording the SEM images of the samples using JEOL JSM-6380LA analytical scanning electron microscopy. Energy dispersive X-ray spectroscopy (EDS) investigations were carried out in order to identify the elemental composition of the species formed on the metal surface after its immersion in 1.0 M sulfuric acid in the presence and absence of inhibitor.

3. Results and discussion

3.1. Potentiodynamic polarization measurements

Potentiodynamic polarization curves for the corrosion of weld aged maraging steel in 1.0 M sulfuric acid solution in the presence of different concentrations of CPOB are shown in Fig. 1. It can be observed that both the cathodic and anodic reactions are suppressed with the addition of CPOB, which suggested that the inhibitor exerted an efficient inhibitory effect both on anodic dissolution of metal and on cathodic hydrogen liberation reaction. Electrochemical parameters such as corrosion potential (E_{corr}), corrosion current density (i_{corr}), and anodic and cathodic Tafel slopes (b_a, b_c) obtained from the polarization measurements are listed in Table 1.

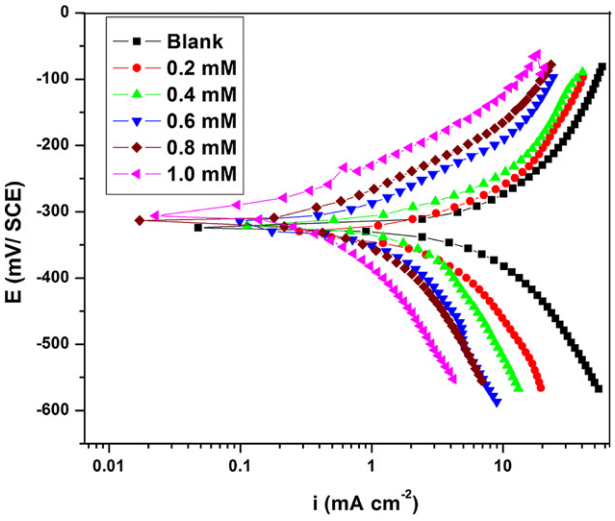

Fig. 1 – Tafel polarization curves for the corrosion of weld aged maraging steel in 1.0 M sulfuric acid containing different concentrations of inhibitor at 30 °C.

The corrosion rate (υ_{corr}), in mm/year, is calculated from following equation [12]:

$$\text{Corrosion rate}(\upsilon_{corr}) = K\frac{i_{corr}}{\rho}EW \quad (1)$$

where K is 3.27×10^{-3}, mm g/μA cm y, a constant that defines the unit for the corrosion rate, i_{corr} is current density in A cm^{-2}, ρ density is in g cm^{-3} and EW is equivalent weight of the alloy. Equivalent weight for alloys was calculated from following equation:

$$EW = \frac{1}{\sum\frac{n_i f_i}{W_i}} \quad (2)$$

where f_i is the mass fraction of the ith element in the alloy, W_i is the atomic weight of the ith element in the alloy and n_i is the valence of the ith element of the alloy. It is usually assumed that the process of oxidation is uniform and does not occur selectively to any component of the alloy.

The inhibition efficiency was calculated from following equation [13]:

$$\eta(\%) = \frac{i_{corr} - i_{corr(inh)}}{i_{corr}} \times 100 \quad (3)$$

where i_{corr} and $i_{corr(inh)}$ signify the corrosion current density in the absence and presence of inhibitors, respectively.

Inhibition efficiency increases with the increase in the inhibitor concentration up to an optimum value. Thereafter the increase in the inhibitor concentration resulted in negligible increase in inhibition efficiency. The maximum quantity of the inhibitor reported in Table 1 corresponds to the optimum concentration of the inhibitor. It is seen from Table 1, that the value of b_c does not change significantly with the increase in inhibitor concentration, which indicates that the addition of CPOB does not change the hydrogen evolution reaction mechanism [14]. Hydrogen evolution reaction has been reported to be generally the dominant local cathodic process in the corrosion of weld aged maraging steel alloy in

Table 1 – Results of potentiodynamic polarization studies on weld aged maraging steel in 1.0 M sulfuric acid containing different concentrations of CPOB.

Temperature (°C)	Inhibitor concentration (mM)	E_{corr} (V/SCE)	b_a (mV dec^{-1})	$-b_c$ (mV dec^{-1})	i_{corr} (mA cm^{-2})	υ_{corr} (mm y^{-1})	η (%)
30	Blank	−323	247	301	8.56	85.9	
	0.2	−322	243	303	3.5	35.1	59.11
	0.4	−319	238	298	2.8	28.1	67.28
	0.6	−314	240	291	2.3	23.1	73.13
	0.8	−312	235	288	1.4	14.0	83.64
	1.0	−309	231	285	0.51	5.1	94.04
35	Blank	−318	276	305	12.8	128.5	
	0.2	−314	271	301	5.7	57.2	55.46
	0.4	−312	274	297	4.6	46.2	64.06
	0.6	−315	267	302	3.7	37.1	71.09
	0.8	−309	259	291	2.2	22.3	82.03
	1.0	−302	263	287	1.4	14.0	89.06
40	Blank	−309	292	307	16.9	169.7	
	0.2	−308	287	310	8.2	82.3	51.47
	0.4	−306	279	299	6.3	63.2	62.72
	0.6	−302	283	292	5.2	52.2	69.23
	0.8	−299	274	295	3.7	37.1	78.10
	1.0	−295	270	288	2.5	25.1	85.20
45	Blank	−308	298	303	19.4	194.8	
	0.2	−305	295	299	9.9	99.4	48.96
	0.4	−307	287	301	8.1	81.3	58.24
	0.6	−299	291	295	6.8	68.3	64.94
	0.8	−297	283	287	5.1	51.2	73.71
	1.0	−293	278	282	3.6	36.1	81.44
50	Blank	−305	312	311	22.1	221.9	
	0.2	−303	314	306	12.3	123.5	44.34
	0.4	−300	307	309	9.6	96.4	56.56
	0.6	−297	302	303	8.4	84.3	61.99
	0.8	−292	297	300	6.7	67.2	69.68
	1.0	−288	294	291	5.1	51.2	76.92

aqueous acidic solutions, via H^+ ion or H_2O molecule reduction, respectively [9]. The amounts of hydrogen evolved by the cathodic reaction are proportional to the corroded amounts of iron. It is also seen from the data that the anodic slope b_a also does not change significantly on increasing the concentration of CPOB, indicating its non-interference in the mechanism of anodic reaction. This indicates that the inhibitive action of CPOB may be considered due to the adsorption and formation of barrier film on the electrode surface. The barrier film formed on the metal surface reduces the probability of both the anodic and cathodic reactions, which results in decrease in corrosion rate [15]. The inhibition efficiency increases with the increase in inhibitor concentration, reaching a maximum value of 94.04% at 1.0 mM.

It can also be seen from Table 1 that there is no appreciable shift in the corrosion potential value (E_{corr}) on the addition of CPOB to the corrosion medium and also on increasing the concentration of CPOB. If the displacement in corrosion potential is more than ±85 mV with respect to corrosion potential of the blank, then the inhibitor can be considered as a cathodic or anodic type [9]. However, the maximum displacement in the present study is ±20 mV, which indicates that CPOB is a mixed type inhibitor. As the concentration of the inhibitor increases from 0.2 mM to 1.0 mM, it is noticed that the corrosion potential shifts slightly toward more positive potential. This indicates that the inhibitor promotes passivation of weld aged maraging steel through adsorption and decreases hydrogen evolution. The increase in the inhibition efficiency with the increase in inhibitor concentration is attributed to the increased surface coverage by the inhibitor molecules as the concentration is increased.

The liberation of hydrogen at the cathodic region can be formulated in three steps as follows [16]:

1. A primary discharge step (Volmer reaction)

$$M + H_3O^+ + e^- \rightarrow MH_{ads} + H_2O \quad (4)$$

2. An electrochemical desorption step (Heyrowsky reaction)

$$MH_{ads} + H_3O^+ + e^- \rightarrow M + H_2 + H_2O \quad (5)$$

3. A recombination step (Tafel reaction)

$$MH_{ads} + MH_{ads} \rightarrow 2M + H_2 \quad (6)$$

The three steps formulated above do not take place as a single step, but combines with another. The presence of inhibitor may prevent the formation of MH_{ads} and suppress

reaction (5) or prevent the electron transfer and to H_3O^+ and suppress reaction (6).

3.2. *Electrochemical impedance spectroscopy (EIS)*

Nyquist plots for the corrosion of weld aged maraging steel in 1.0 M sulfuric acid solution in the presence of different concentrations of CPOB are shown in Fig. 2. It can be observed from the figure that the diameter of the semicircle increases with the increase in the concentration of CPOB, indicating a decrease in the corrosion rate of the alloy sample. It is seen from the Fig. 2 that the impedance spectra did not present perfect semicircles. The depressed semicircle is often attributed to the surface roughness, dislocations and distribution of the active sites or adsorption of inhibitors [5]. The impedance data were analyzed using an equivalent circuit (EC) that tentatively models the physical processes occurring at the metal–electrolyte interface. The EC, as shown in Fig. 3 was used to simulate the measured impedance data for the corrosion of the alloy in 0.1 M sulfuric acid. The circuit fitment was done by ZSimpWin software of version 3.21. The Nyquist curve contains a single semicircle capacitive loop. The equivalent circuit model shown in Fig. 3(a) was used for the corrosion of the alloy in the absence of CPOB. The EC consists of the electrolyte solution resistance (R_s), charge-transfer resistance (R_{ct}) and constant-phase element (*CPE*, Q). A constant-phase element (*CPE*) is employed instead of the double-layer capacitance (C_{dl}) to describe the non-homogeneities in the system. R_{ct} is a resistance to the corrosion process. That resistance can be present as the charge-transfer resistance at the metal/oxide film interface, the resistance of the oxide film, and/or the charge-transfer resistance at the oxide film/solution interface [17]. The *CPE* impedance (Z_{CPE}) is given by the expression:

$$Z_{CPE} = \frac{1}{Q} \times \frac{1}{(j\omega)^n} \tag{7}$$

where Q is the *CPE* coefficient, n is the *CPE* exponent (phase shift), ω is the angular frequency ($\omega = 2\pi f$, where f is the AC frequency) and j is the imaginary unit. When the value of n is 1, the *CPE* behaves like an ideal double-layer capacitance (C_{dl}). The correction of capacitance to its real values is calculated from the expression [18]:

$$C_{dl} = Q(\omega_{max})^{n-1} \tag{8}$$

where ω_{max} is the frequency at which the imaginary part of impedance ($-Z_i$) has a maximum.

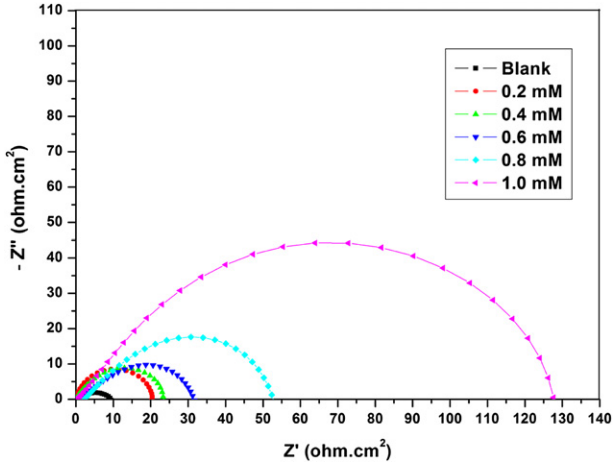

Fig. 2 – Nyquist plots for the corrosion of weld aged maraging steel in 1.0 M sulfuric acid containing different concentrations of inhibitor at 30 °C.

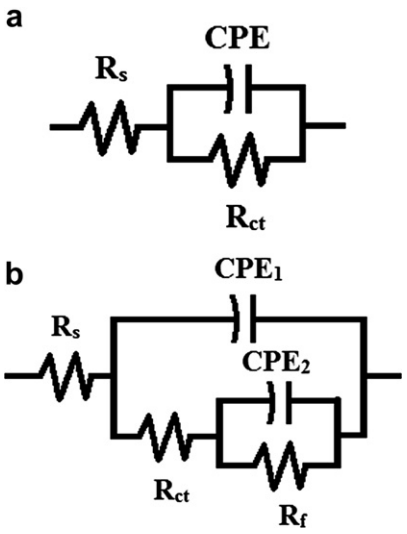

Fig. 3 – Equivalent circuit used to fit the experimental EIS data for the corrosion of weld aged maraging steel specimen in 1.0 sulfuric acid at 30 °C (a) in the absence of inhibitor and (b) in the presence of inhibitor.

However, the impedance plots recorded for the corrosion of the alloy in the presence of CPOB were modeled by using the equivalent circuit depicted in Fig. 3(b), which consists of the R_s, C_{dl}, C_f (film capacitance) and R_f (film resistance). The R_{ct}, R_f, C_{dl} and C_f were determined by the analysis of Nyquist plots and their values are given in Table 2. The results show that the values of C_{dl} and C_f decrease, while the values of R_{ct} and R_f increase with the increase in the concentration of CPOB, suggesting that the amount of the inhibitor molecules adsorbed on the electrode surface increases as the concentration of CPOB increases. The decrease in C_{dl} and C_f could be attributed to the decrease in local dielectric constant and/or an increase in the thickness of the electrical double layer, signifying that the CPOB molecules act by adsorption at the interface of metal/solution. The change in R_{ct}, R_f, C_{dl} and C_f values are caused by the gradual replacement of adsorbed water molecules by the inhibitor molecules on the metal surface. The R_{ct} was used to calculate the inhibition efficiency (η%) from the following equation [19]:

$$\eta(\%) = \frac{R_{ct(inh)} - R_{ct}}{R_{ct(inh)}} \times 100 \tag{9}$$

where $R_{ct(inh)}$ and R_{ct} are the charge-transfer resistances obtained in inhibited and uninhibited solutions, respectively. Thus, when the inhibitor concentration increases, more inhibitor molecules will be adsorbed on the surface through the active centers in the compound which may be double

Table 2 – EIS data of weld aged maraging steel in 1.0 M sulfuric acid containing different concentrations of CPOB.

Temperature (°C)	Inhibitor concentration (mM)	R_{ct} (Ω cm^2)	C_{dl} (mF cm^{-2})	R_f (Ω cm^2)	C_f (mF cm^{-2})	η (%)
30	Blank	8.56	22.5			
	0.2	20.1	13.6	1.67	1.3	57.4
	0.4	24.7	8.2	2.05	0.79	65.3
	0.6	29.8	6.1	2.48	0.58	71.3
	0.8	48.1	3.7	3.75	0.36	82.2
	1.0	125.7	1.7	5.1	0.16	93.1
35	Blank	6.7	26.7			
	0.2	14.8	17.5	1.23	1.69	54.7
	0.4	18.6	11.3	1.55	1.09	64.0
	0.6	22.5	8.6	1.87	0.83	70.2
	0.8	35.2	6.0	3.20	0.64	80.9
	1.0	53.2	5.9	3.68	0.57	87.4
40	Blank	5.1	28.2			
	0.2	10.1	22.6	0.84	2.37	49.5
	0.4	13.0	24.5	1.08	2.18	60.7
	0.6	16.4	13.8	1.36	1.34	68.9
	0.8	23.3	8.4	2.12	0.81	78.1
	1.0	37.0	6.5	3.07	0.62	86.2
45	Blank	4.1	30.8			
	0.2	7.9	27.5	0.68	2.66	48.1
	0.4	9.7	23.4	0.81	2.25	58.1
	0.6	12.4	19.2	1.03	1.86	66.9
	0.8	14.9	12.4	1.17	1.20	72.4
	1.0	23	8.7	1.91	0.84	82.1
50	Blank	3.5	36.8			
	0.2	6.6	33.1	0.55	3.18	46.9
	0.4	7.8	27.4	0.65	2.64	55.1
	0.6	9.6	23.2	0.80	2.24	63.5
	0.8	12.0	17.3	1.05	1.67	70.8
	1.0	15.5	15.2	1.29	1.47	77.4

bonds or heteroatom oxygen, which leads to the increase in film thickness and decrease in hydrogen evolution. The inhibitor molecule CPOB has the most electron rich environment in phenyl group due to resonance of π-electrons of double bonds that can be adsorbed well on the sample surface. Also methoxy and carbonyl groups are electron donating groups containing oxygen atom as an active site.

The Bode plot for the corrosion of the alloy in the presence of different concentrations of CPOB is shown in Fig. 4. The high frequency (*HF*) limits correspond to R_s (Ω), while the lower frequency (*LF*) limits correspond to ($R_{ct} + R_s$), which are associated with the dissolution processes at the interface. Phase angle increases with the increase in the concentrations of CPOB in sulfuric acid medium. This might be attributed to the decrease in the capacitive behavior on the metal surface due to decrease in the dissolution rate of the metal. The difference between the *HF* limit and *LF* limit, corresponding to R_{ct} value for the inhibited system in the Bode plot increases with increase in the concentration of CPOB [20]. At the highest inhibitor concentration of 1.0 mM, the inhibition efficiency was reached at 93.1%. The impedance results are in good agreement with the results achieved from potentiodynamic polarization studies.

3.3. *Effect of temperature*

The results of potentiodynamic polarization and electrochemical impedance spectroscopy given in Tables 1 and 2 indicate that the inhibition efficiency of CPOB decreases with increase in temperature. It is also seen from the data in the Tables that the increase in solution temperature, does not alter the corrosion potential (E_{corr}), anodic Tafel slope (b_a) and cathodic Tafel slope (b_c) values significantly. This indicates that the increase in temperature does not change the mechanism of corrosion reaction. However, i_{corr} and hence the corrosion rate of the specimen increases with the increase in

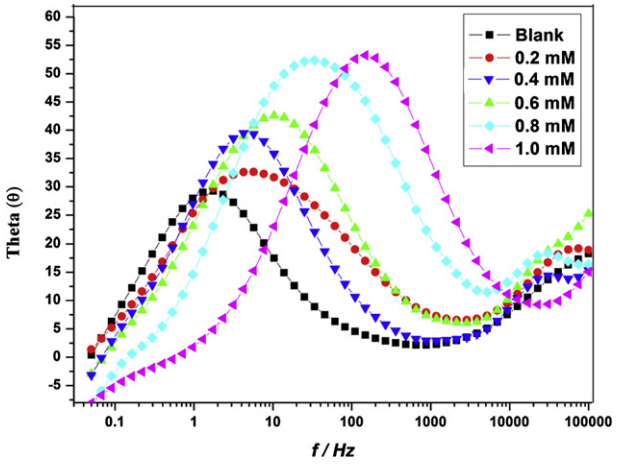

Fig. 4 – Bode plots for the corrosion of weld aged maraging steel specimen in 1.0 M sulfuric acid containing different concentrations of inhibitor at 30 °C.

temperature for both blank and inhibited solutions. The decrease in inhibition efficiency with the increase in temperature may be attributed to the higher dissolution rates of weld aged maraging steel at elevated temperature and also a possible desorption of adsorbed inhibitor due to the increased solution agitation resulting from higher rates of hydrogen gas evolution. The higher rate of hydrogen gas evolution may also reduce the ability of the inhibitor to be adsorbed on the metal surface. The decrease in inhibition efficiency with the increase in temperature is also suggestive of physisorption of the inhibitor molecules on the metal surface [21].

The apparent activation energy (E_a) for the corrosion process in the presence and absence of the inhibitor was calculated using Arrhenius law Equation [5]:

$$\ln(\upsilon_{corr}) = B - \frac{E_a}{RT} \quad (10)$$

where B is a constant which depends on the metal type, R is the universal gas constant and T is the absolute temperature. The plot of $\ln(\upsilon_{corr})$ versus reciprocal of absolute temperature ($1/T$) gives a straight line with slope $=-E_a/R$, from which, the activation energy values for the corrosion process were calculated. The Arrhenius plots for the corrosion of weld aged maraging steel in the presence of different concentrations of CPOB in 1.0 M sulfuric acid are shown in Fig. 5.

The entropy of activation ($\Delta H^{\#}$) and enthalpy of activation ($\Delta S^{\#}$) for the corrosion of alloy were calculated from the transition state theory Equation [21]:

$$\upsilon_{corr} = \frac{RT}{Nh}\exp\left(\frac{\Delta S^{\#}}{R}\right)\exp\left(\frac{-\Delta H^{\#}}{R}\right) \quad (11)$$

where h is Plank's constant, and N is Avagadro's number. The plots of $\ln(\upsilon_{corr}/T)$ versus $1/T$ in 1.0 M H_2SO_4 acid in the presence of different concentrations of CPOB are shown in Fig. 6. The calculated values of E_a, $\Delta H^{\#}$ and $\Delta S^{\#}$ are given in Table 3.

The data in the Table 3 show that the values of E_a for the corrosion of weld aged maraging steel in 1.0 M sulfuric acid in the presence of CPOB are higher than those in the uninhibited

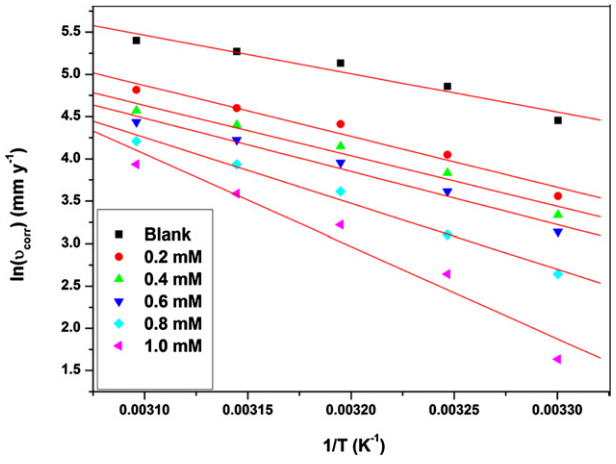

Fig. 5 – Arrhenius plots for the corrosion of weld aged maraging steel in 1.0 M sulfuric acid containing different concentrations of inhibitor.

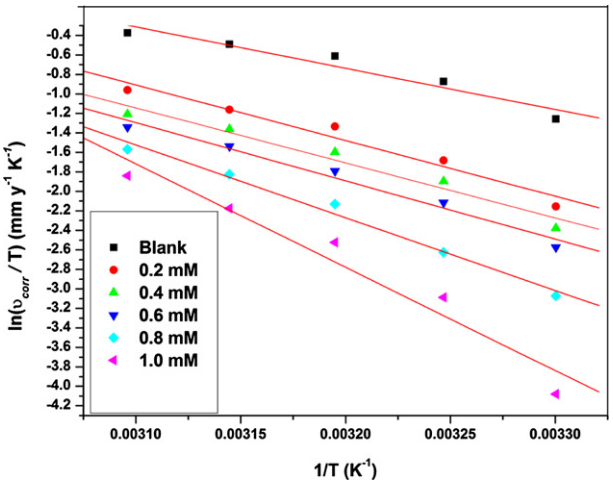

Fig. 6 – Plots of $\ln(\upsilon_{corr}/T)$ versus $1/T$ for the corrosion of weld aged maraging steel in 1.0 M sulfuric acid containing different concentrations of inhibitor.

medium. The increase in the E_a values, with increasing inhibitor concentration indicates the increase in energy barrier for the corrosion reaction, with the increasing concentrations of the inhibitor [14]. It is also indicated that the whole process is controlled by surface reaction, since the activation energies of the corrosion process are above 20 kJ mol^{-1}. The adsorption of the inhibitor on the electrode surface leads to the formation of a physical barrier between the metal surface and the corrosion medium, blocking the charge transfer, and thereby reducing the metal reactivity in the electrochemical reactions of corrosion.

The large negative values of entropy of activation ($\Delta S^{\#}$) in the absence and presence of inhibitor imply that the activated complex in the rate determining step represents an association rather than dissociation, resulting in a decrease in randomness on going from the reactants to the activated complex [20].

3.4. *Adsorption isotherm*

The information on the interaction between the inhibitor molecules and the metal surface can be provided by adsorption isotherm. The adsorption of CPOB molecule on the metal

Table 3 – Activation parameters for the corrosion of weld aged maraging steel in 1.0 M sulfuric acid containing different concentrations of inhibitor.

Inhibitor concentration (mM)	E_a (kJ^{-1} mol^{-1})	$\Delta H^{\#}$ (kJ^{-1} mol^{-1})	$\Delta S^{\#}$ (J mol^{-1} K^{-1})
Blank	37.80	35.20	−91.07
0.2	51.71	47.46	−57.98
0.4	49.48	47.00	−61.39
0.6	52.20	49.60	−22.97
0.8	64.61	62.02	−17.99
1.0	90.70	88.10	−11.24

surface can occur either through donor–acceptor interaction between the unshared electron pairs and/or π-electrons of inhibitor molecule and the vacant d-orbitals of the metal surface atoms, or through electrostatic interaction of the inhibitor molecules with already adsorbed sulfate ions. The adsorption bond strength is dependent on the composition of the metal, corrodent, inhibitor structure, concentration and orientation as well as temperature [6]. The adsorption of an organic adsorbate at metal/solution interface can be presented as a substitution adsorption process between the organic molecules in aqueous solution (Org_{aq}), and the water molecules on metallic surface (H_2O_{ads}), as given below [22]:

$$Org_{(sol)} + \chi H_2O \leftrightarrow Org_{(ads)} + \chi H_2O \quad (12)$$

where χ, the size ratio, is the number of water molecules displaced by one molecule of organic inhibitor. χ is assumed to be independent of coverage or charge on the electrode.

The surface coverage (θ) was calculated from potentiodynamic polarization data using the equation [21]:

$$\theta = \frac{\eta(\%)}{100} \quad (13)$$

where $\eta(\%)$ is the percentage inhibition efficiency. The values of θ at different concentrations of inhibitor in the solution (C_{inh}) were applied to various isotherms including Langmuir, Temkin, Frumkin and Flory–Huggins isotherms. It was found that the data fitted best with the Langmuir adsorption isotherm, which is given by the relation,

$$\frac{C_{inh}}{\theta} = C_{inh} + \frac{1}{K} \quad (14)$$

where K is the adsorption/desorption equilibrium constant, C_{inh} is the corrosion inhibitor concentration in the solution, and θ is the surface coverage.

The plot of C_{inh}/θ versus C_{inh} gives a straight line with an intercept of $1/K$. The Langmuir adsorption isotherms for the adsorption of CPOB on the maraging steel surface are shown in Fig. 7. The plots are linear, with an average correlation coefficient of 0.991.

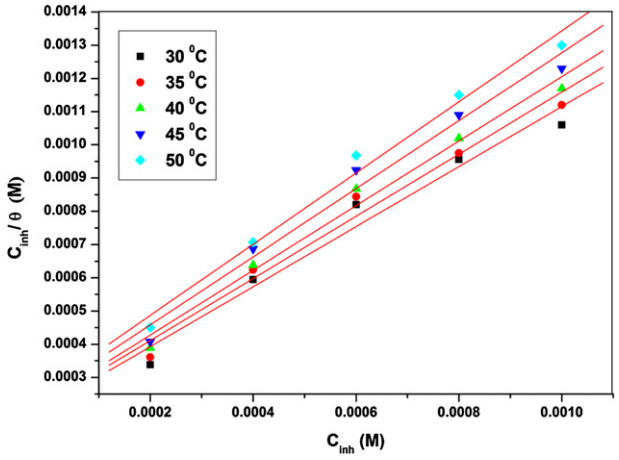

Fig. 7 – Langmuir adsorption isotherms for the adsorption of CPOB on weld aged maraging steel in 1.0 M sulfuric acid at different temperatures.

The standard free energy of adsorption, (ΔG^0_{ads}) was calculated using the relation [9]:

$$K = \frac{1}{55.5}\exp\left(\frac{-\Delta G^0_{ads}}{RT}\right) \quad (15)$$

where the value 55.5 is the concentration of water in solution in mol dm^{-3}, R is the universal gas constant and T is absolute temperature. Standard enthalpy of adsorption (ΔH^0_{ads}) and standard entropies of adsorption (ΔS^0_{ads}) were obtained from the plot of (ΔG^0_{ads}) versus T according to the thermodynamic equation [13]:

$$\Delta G^0_{ads} = \Delta H^0_{ads} - T\Delta S^0_{ads} \quad (16)$$

The plot of (ΔG^0_{ads})/T is shown in Fig. 8. The thermodynamic data obtained for the adsorption of CPOB on the surface the alloy are tabulated in Table 4. The negative sign of ΔH^0_{ads} in sulfuric acid solution indicates that the adsorption of inhibitor molecules is an exothermic process. Generally, an exothermic adsorption process signifies either physisorption or chemisorptions while endothermic process is attributable unequivocally to chemisorption. Typically, the standard enthalpy of physisorption process is less negative than 41.86 kJ mol^{-1}, while that of chemisorptions process approaches to −100 kJ mol^{-1} [23]. In the present study the value of ΔH^0_{ads} is −10.38 kJ mol^{-1}, which shows that the adsorption of CPOB on weld aged maraging steel involves physisorption phenomenon. The negative values of ΔG^0_{ads} indicate the spontaneity of the adsorption process and the stability of the adsorbed layer on the metal surface. Generally the values of ΔG^0_{ads} less than −20 kJ mol^{-1} are consistent with physisorption, while those greater than −40 kJ mol^{-1} are corresponding to chemisorptions [24,25]. The calculated values of ΔG^0_{ads} obtained in this study range between −31.42 kJ mol^{-1} and −32.82 kJ mol^{-1}, indicating both physical and chemical adsorption behavior of CPOB on the metal surface. These values indicate that the adsorption process may involve complex interactions involving both physical and chemical adsorption of the inhibitor [18]. The fact that both ΔG^0_{ads} and inhibition efficiency decrease with the increase in temperature, indicates that the adsorption of CPOB on the weld aged maraging steel surface in sulfuric acid are not favored at high temperature and hence can be considered to

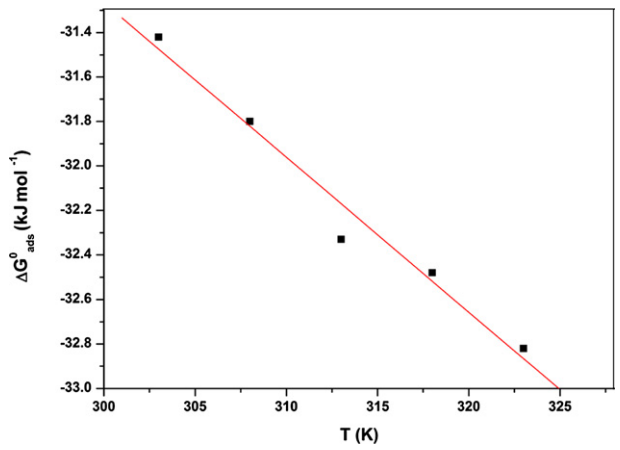

Fig. 8 – The plot of (ΔG^0_{ads})/T for the adsorption of CPOB on weld aged maraging steel in 1.0 M sulfuric acid.

Table 4 – Thermodynamic parameters for the adsorption of CPOB on weld aged maraging steel surface in 1.0 M sulfuric acid.

Temperature (°C)	$-\Delta G^0_{ads}$ (kJ mol^{-1})	ΔH^0_{ads} (kJ mol^{-1})	ΔS^0_{ads} (J mol^{-1} K^{-1})
30	31.42	−10.38	−69.6
35	31.80		
40	32.33		
45	33.48		
50	32.82		

be predominantly physisorption [26]. The ΔS^0_{ads} value is large and negative; indicating that decrease in disordering takes place on going from the reactant to the alloy adsorbed species. This can be attributed to the fact that adsorption is always accompanied by decrease in entropy [26].

3.5. *Mechanism of corrosion inhibition*

The inhibitive effect of CPOB on the corrosion of weld aged maraging steel can be accounted for on the basis of its adsorption on the alloy surface. The adsorption of CPOB molecules on the metal surface can be attributed to the presence of electronegative elements like oxygen and chlorine and also to the presence of π-electron cloud in the benzene ring of the molecule. The adsorption mechanism for a given inhibitor depends on factors, such as the nature of the metal, the corrosive medium, the pH, and the concentration of the inhibitor as well as the functional groups present in its molecule, since different groups are adsorbed to different extents. Weld aged maraging steel consists of segregated alloying elements along the grain boundaries. Since these segregations have different composition, their electrochemical behavior is expected to be different from that of the matrix [27]. Also, the lattice mismatch between the precipitate and the matrix causes strain field around the segregated precipitates. These strain fields in combination with the galvanic effect due to the composition difference leads to the enhanced corrosion of weld aged maraging steel in acid medium. Considering the inhomogeneous nature, the surface of the alloy is generally characterized by multiple adsorption sites having different activation energies and enthalpies of adsorption. Inhibitor molecules may thus be adsorbed more readily at surface active sites having suitable adsorption enthalpies.

To understand the mechanism of inhibition and the effect of inhibitor in aggressive acidic environment, some knowledge of interaction between the protective compound and the metal surface is required. Many organic corrosion inhibitors have at least one polar unit with a heteroatom; this polar unit is regarded as the reaction center for the adsorption process. Furthermore, the size, orientation, shape and electric charge on the molecule determine the degree of adsorption and hence the effectiveness of inhibitor. On the other hand, iron is well known for its coordination affinity to ligands possessing heteroatom. Increase in inhibition efficiencies with increase in inhibitor concentration shows that the inhibition action is due to the adsorption on the maraging steel surface. Adsorption may take place by organic molecules at metal/solution interface due to electrostatic attraction between the charged molecules and charged metal, interaction of unshared electron pairs in the molecule with the metal, interaction of π-electrons with the metal or the combination of the above.

In acidic solution, the following mechanism is proposed for the corrosion of iron and steel [7].

$$Fe + H_2O \leftrightarrow FeOH_{ads} + H^+ + e^- \quad (17)$$

$$FeOH_{ads} \rightarrow FeOH^+ + e^- (\text{rate determining step}) \quad (18)$$

$$FeOH^+ + H^+ \leftrightarrow Fe^{2+} + H_2O \quad (19)$$

The cathodic hydrogen evolution follows the steps:

$$Fe + H^+ \leftrightarrow (FeH^+)_{ads} \quad (20)$$

$$(FeH^+)_{ads} + e^- \leftrightarrow (FeH)_{ads} \quad (21)$$

$$(FeH)_{ads} + H^+ + e^- \rightarrow Fe + H_2 \quad (22)$$

In the aqueous acidic solutions, CPOB exists partly in the form of protonated species and partly as neutral molecules. Generally, two modes of adsorption could be considered. It is well known that steel surface bears a positive charge in acid solutions [6,28,29]. The adsorption of the negatively charged

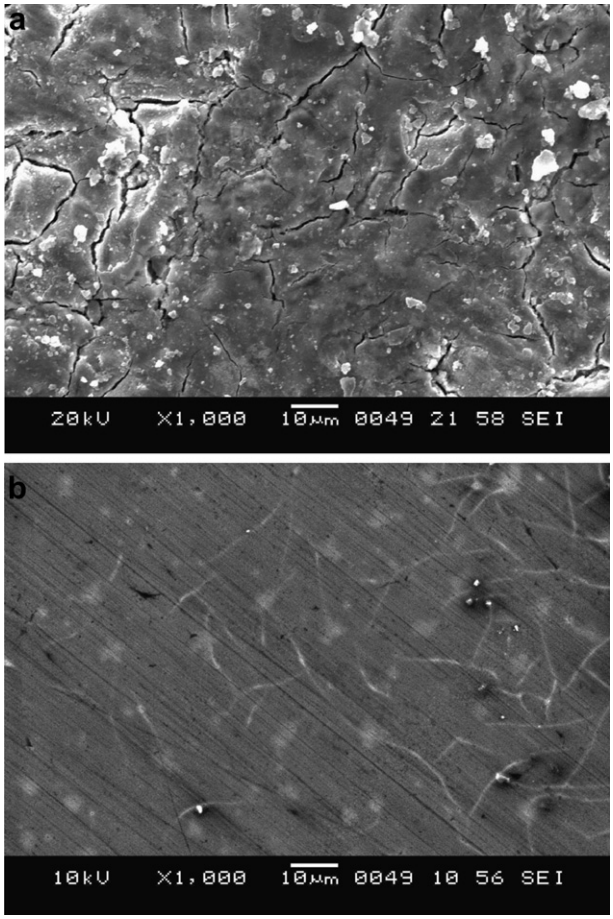

Fig. 9 – SEM images of the weld aged maraging steel after immersion in 1.0 M sulfuric acid (a) in the absence and (b) in the presence of CPOB.

sulfate ions renders the metal surface negative and susceptible for the physical adsorption of the positively charged protonated inhibitor species. Therefore, the adsorption of protonated species would be through electrostatic attraction between the positively charged inhibitor molecule and the negatively charged sulfate ions adsorbed on the metal surface, resulting in physisorption. The neutral inhibitor molecules may occupy the vacant adsorption sites on the metal surface through the chemisorption mode involving the displacement of water molecules from the metal surface and sharing of electrons by the heteroatoms like oxygen and/or chlorine with iron. The presence of ATPI in the protonated form and the presence of negative charge centers on the molecule are also responsible for the mutual interaction of inhibitor molecules on the alloy surface. This is reflected in the deviation of slopes of Langmuir adsorption isotherms as discussed in the previous section.

3.6. SEM/EDS studies

In order to differentiate between the surface morphology and to identify the composition of the species formed on the metal surface after its immersion in 1.0 M sulfuric acid in the absence and in the presence of CPOB, SEM/EDS investigations were carried out. Fig. 9(a) represents SEM image of the corroded weld aged maraging steel sample. The corroded surface shows detachment of particles from the surface. The corrosion of the alloy may be predominantly attributed to the inter-granular corrosion assisted by the galvanic effect between the precipitates and the matrix along the grain boundaries. Fig. 9(b) represents SEM image of weld aged maraging steel after the corrosion tests in a medium of sulfuric acid containing 1.0 mM of CPOB. The image clearly shows a smooth surface due to the adsorbed layer of inhibitor molecules on the alloy surface, thus protecting the metal from

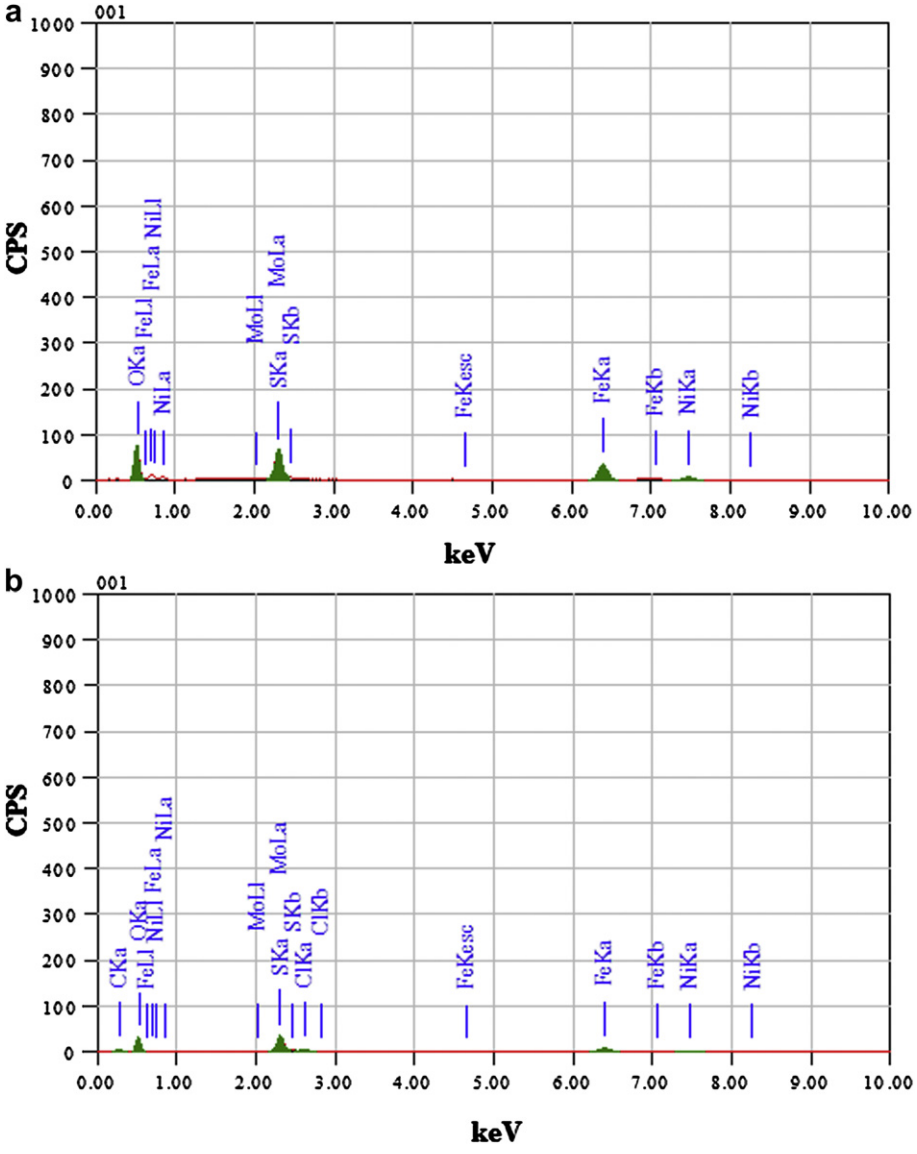

Fig. 10 – EDS spectra of the weld aged maraging steel after immersion in 1.0 M sulfuric acid (a) in the absence and (b) in the presence of CPOB.

corrosion. EDS investigations were carried out in order to identify the composition of the species formed on the metal surface in 1.0 M sulfuric acid in the absence and presence of CPOB. The corresponding EDS profile analyses for the selected areas on the SEM images of Fig. 9(a) and (b) are shown in Fig. 10(a) and (b), respectively. The atomic percentage of the elements found in the EDS profile for corroded metal surface was 12.29% Fe, 3.47 Ni, 4.32% Mo, 73.65% O, 1.75% Co and 6.57% S and indicated that iron oxide is existing in this area. These elemental composition prove that the corrosion of weld aged maraging steel through the formation of oxide layer. The atomic percentage of the elements found in the EDS profile for inhibited metal surface was 4.07% Fe, 0.62% Ni, 1.85% Mo, 52.90% O, 1.03% Cl, 34.21% C and 5.31% S and indicated the formation of inhibitor film in this area. The elemental compositions mentioned above were mean values of different regions.

4. Conclusions

- The CPOB acts as a mixed type inhibitor, which affects both the anodic dissolution of weld aged maraging steel and cathodic hydrogen evolution reactions.
- The inhibition efficiency of CPOB decreases with the increase in concentration of CPOB and decreases with the increase in temperature.
- The adsorption of CPOB was found to follow the Langmuir's adsorption isotherm. The calculated thermodynamic parameters indicate that the inhibition process occurs via physical adsorption.
- The results obtained from EIS and polarization studies are in a good agreement.
- The SEM/EDX observation proves that the inhibition of corrosion is due to formation of an adsorbed passive film on the metal surface.

REFERENCES

[1] Menapace C, Lonardelli I, Molinari A. Phase transformation in a nanostructured M300 maraging steel obtained by SPS of mechanically alloyed powders. J Therm Anal Calorim 2010; 101:815.

[2] Stiller K, Danoix F, Bostel A. Investigation of precipitation in a new maraging stainless steel. Appl Surf Sci 1996;94:326.

[3] Poornima T, Nayak J, Shetty AN. Corrosion of aged and annealed 18 Ni 250 grade maraging steel in phosphoric acid medium. Int J Electrochem Sci 2010;5:56–71.

[4] Rezek J, Klein IE, Yhalom J. Electrochemical properties of protective coatings on maraging steel. Corros Sci 1997;39(2): 385.

[5] Poornima T, Nayak J, Shetty AN. 3, 4-Dimethoxy benzaldehyde thiosemicarbazone as corrosion inhibitor for aged 18Ni 250 grade maraging steel in 0.5 M sulfuric acid. J Appl Electrochem 2011;41:223–33.

[6] Poornima T, Nayak J, Shetty AN. Effect of 4-(N,N-diethylamino)benzaldehyde thiosemicarbazone on the corrosion of aged 18 Ni 250 grade maraging steel in phosphoric acid solution. Corrosion Sci 2011;53:3688–96.

[7] Obot IB, Obi-Egbedi NO, Eseola AO. Anticorrosion potential of 2-mesityl-1H-imidazo[4,5-f][1,10]-phenanthroline on mild steel in sulfuric acid solution: experimental and theoretical study. Ind Eng Chem Res 2011;50:2098–110.

[8] Tao Z, Zhang S, Li W, Hou B. Adsorption and inhibitory mechanism of 1H-1,2,4-triazol-l-yl-methyl-2-(4-chlorophenoxy) acetate on corrosion of mild steel in acidic solution. Ind Eng Chem Res 2011;50:6082–8.

[9] Fekry AM, Ameer MA. Corrosion inhibition of mild steel in acidic media using newly synthesized heterocyclic organic molecules. Int J Hydrogen Energy 2010;35:7641–51.

[10] Fun HK, Shahani T, Garudachari B, Arun IM, Satyganarayan MN. 2-(4-Chlorophenyl)-2-oxoethyl benzoate. Acta Crystallog Sect E 2011;67:1802.

[11] Le ZG, Xie ZB, Xu JP. One-pot synthesis of phenacyl esters from acetophenone, [Bmim]Br_3, and potassium salts of carboxylic acids under solvent-free conditions. Synth Commun 2009;39:743–7.

[12] Dean SW. Standard practice for calculation of corrosion rates and related information from electrochemical measurements. Norm ASTM G102; 1999. p. 2–3.

[13] Prabhu RA, Shanbhag AV, Venkatesha TV. Influence of tramadol [2-[(dimethylamino)methyl]-1-(3- methoxyphenyl) cyclohexanol hydrate] on corrosion inhibition of mild steel in acidic media. J Appl Electrochem 2007;37:491–7.

[14] Avci G. Corrosion inhibition of indole-3-acetic acid on mild steel in 0.5 M HCl. Colloids Surf A 2008;317:730–6.

[15] Li W, He Q, Zhang S, Pei C, Hou B. Some new triazole derivatives as inhibitors for mild steel corrosion in acidic medium. J Appl Electrochem 2008;38:289–95.

[16] Fekry AM, Ameer MA. Electrochemical investigation on the corrosion and hydrogen evolution rate of mild steel in sulphuric acid solution. Int J Hydrogen Energy 2011;36: 11207–15.

[17] Yagan A, Pekmez NO, Yıldız A. Electrochemical synthesis of poly (N-methylaniline) on an iron electrode and its corrosion performance. Electrochim Acta 2008;53:5242–51.

[18] Machnikova E, Kenton WH, Hackerman N. Corrosion inhibition of carbon steel in hydrochloric acid by furan derivatives. Electrochim Acta 2008;53:6024–32.

[19] Wang X, Yang H, Wang F. A cationic gemini-surfactant as effective inhibitor for mild steel in HCl solutions. Corros Sci 2010;52:1268–76.

[20] Fouda AS, Heakal FE, Radwan MS. Role of some thiadiazole derivatives as inhibitors for the corrosion of C-steel in 1 M H_2SO_4. J Appl Electrochem 2009;39:391–402.

[21] Geetha MP, Nayak J, Shetty AN. Corrosion inhibition of 6061Al-15vol.pct.SiC(p) composite and its base alloy in a mixture of sulphuric acid and hydrochloric acid by 4-(N,N-dimethylamino) benzaldehyde thiosemicarbazone. Mater Chem Phys 2011;125:628–40.

[22] Tao Z, Zhang S, Li W, Hou B. Adsorption and corrosion inhibition behavior of mild steel by one derivative of benzoic-triazole in acidic solution. Ind Eng Chem Res 2010; 49:2593–9.

[23] Singh AK, Quraishi MA. Effect of cefazolin on the corrosion of mild steel in HCl solution. Corros Sci 2010;52:152–60.

[24] Ameer MA, Fekry AM. Inhibition effect of newly synthesized heterocyclic organic molecules on corrosion of steel in alkaline medium containing chloride. Int J Hydrogen Energy 2010;35:11387–96.

[25] Ameer MA, Fekry AM, Ghoneim AA, Attaby FA. Electrochemical corrosion inhibition of steel in alkaline chloride solution. Int J Electrochem Sci 2010;5:1847–61.

[26] Sanaa T. Arab Inhibition action of thiosemicabazone and some of it is r-substituted compounds on the corrosion of iron-base metallic glass alloy in 0.5 M H_2SO_4 at 30 °C. Mater Res Bull 2008;43:510–21.

[27] Fragnani A, Trabanelli G. Influence of organic additives on the corrosion of iron-based amorphous alloys in dilute sulfuric acid solution. Corrosion 1999;55:653–60.
[28] Mu GN, Li XM, Li F. Synergistic inhibition between o-phenanthroline and chloride ion on cold rolled steel corrosion in phosphoric acid. Mater Chem Phys 2004;86:59–68.
[29] Wang L. Evaluation of 2-mercaptobenzimidazole as corrosion inhibitor for mild steel in phosphoric acid. Corrosion Sci 2001;43:2281–9.